# An experimental investigation of the EMI-based SHM of RC structure under dynamic loading

George M. Sapidis  $^{1,0000-0002-0240-5699}$ , Maria C. Naoum  $^{1,0000-0002-2262-8267}$ , Nikos A. Papadopoulos  $^{1,0009-0007-1183-4616}$ , Maristella E. Voutetaki  $^{2,0000-0003-2420-9696}$  and Theodoros C. Rousakis  $^{1,0000-0002-6384-1451}$ 

<sup>1</sup> Laboratory of Reinforced Concrete and Seismic Design of Structures, Civil Engineering Department, School of Engineering, Democritus University of Thrace – Xanthi 67100, Greece
<sup>2</sup> 2Structural Science and Technology Division, Architectural Engineering Department, School of Engineering, Democritus University of Thrace – Xanthi 67100, Greece
gsapidis@civil.duth.gr

Abstract. Buildings featuring vertical greenery typically provide substantial ecological, aesthetic, and economic advantages. However, the increased loads associated with the planting jeopardize the structural integrity, particularly in areas of significant seismic activity. Consequently, Structural Health Monitoring (SHM) methodologies, such as electro-mechanical impedance (EMI), are utilized to enhance the safety of structures. While the efficacy of the EMI method for SHM in reinforced concrete (RC) structural elements subjected to quasi-static loading sequences has been thoroughly examined in the literature, a notable research gap exists concerning its investigation under dynamic loading conditions. This study conducts an experimental inquiry into the feasibility of the EMI method for damage identification in a one-bay, one-story RC space frame structure subjected to earthquake vibrations. Consequently, a shaking table was employed to stimulate the RC frame with gradually increasing ground excitation, in which piezoelectric patches are strategically integrated at carefully selected positions. The incorporated PZT sensors enable prompt assessment of earthquake-induced damage to the RC frame. The experimental results indicate that the EMI method proficiently and swiftly detected damage formation within the RC frame.

**Keywords:** Structural Health Monitoring (SHM), Electro-Mechanical Impedance (EMI), damage diagnosis, dynamic loading, Reinforced Concrete (RC) frame.

# 1 Introduction

The renovation of existing buildings to improve energy efficiency has recently gained significant popularity, due to the environmental and economic consequences of climate change. Furthermore, the implementation of green politics, along with the substantial ecological, aesthetic, and financial benefits of buildings featuring vertical greenery, has increased their popularity in recent times. Nevertheless, the escalated loads related to the planting pose a risk to the structural integrity, especially in regions with heightened seismic activity. The external loads of buildings with vertical greenery are transferred either directly to the building's slab or via the infill walls, as depicted in Fig. 1. However, these loads will ultimately impose stress on the vertical structural elements, such as RC columns. Furthermore, during a seismic event, they will increase the inertial mass of the building, thereby augmenting the total base shear. Additionally, the current building stock is more susceptible due to its construction in accordance with outdated building regulations. Therefore, the assessment of the structural integrity has become of utmost importance.

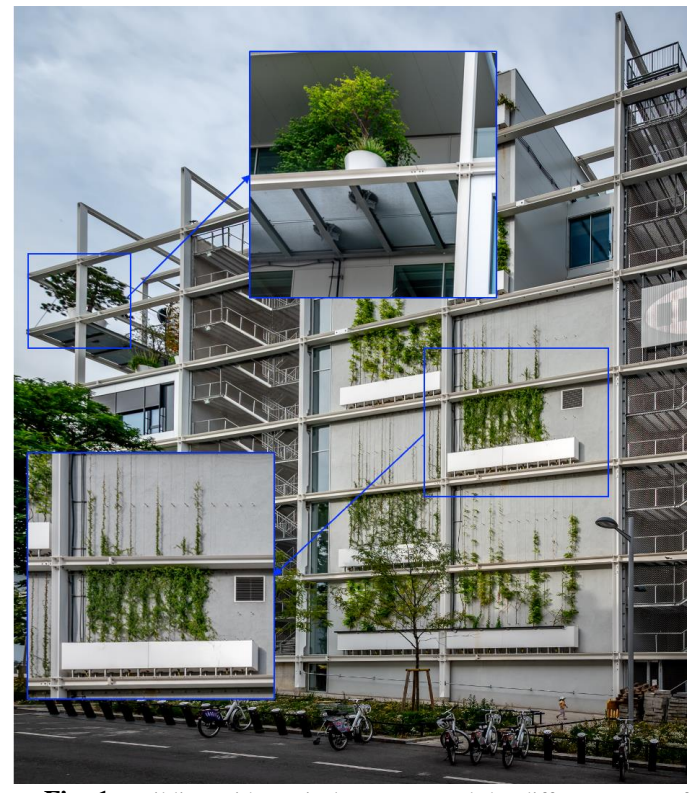


**Fig. 1.** Building with vertical greenery and the different types of plant-associated external loads.

Visual inspection by highly skilled structural engineers is the conventional method for assessing structural integrity. Although visual inspections provided critical information, they face severe drawbacks regarding inaccessible or coated structural members and prompt diagnosis of structural damage. Furthermore, the energy renovation of existing structures has intensified the challenges of visual inspections, as a greater proportion of Reinforced Concrete (RC) members are inaccessible due to the use of insulating materials. In contrast, newly developed Structural Health Monitoring (SHM) methods, with real-time capabilities, enable continuous inspection of RC structures. Li et al. utilized a PZT-enabled SHM approach for the assessment of damage in an RC planting balcony over a period of approximately seven months [1]. The proposed SHM scheme produces promising results; however, temperature compensation is conducted to account for the effects of ambient temperature on the PZT transducers. Therefore, SHM methods have gained research interest as essential tools for assessing the structural integrity of newly constructed or existing buildings [2].

Over the past decades, numerous SHM techniques have emerged, including Acoustic Emissions [3, 4], Guided Waves [5, 6], laser scanning [7, 8], infrared thermography [9, 10], digital imaging and image correlation techniques [11–14], and the Electro-Mechanical Impedance (EMI) method. According to the extensive literature, the EMI method constitutes a localized SHM technique, capable of ensuring prompt diagnosis of crack formation in RC members [15–18]. Among the various SHM techniques, the EMI method has garnered substantial recognition as a promising approach for continuous structural integrity assessment of RC structures. This is attributed to its unique integrated functionality, whereby a single piezoelectric transducer functions concurrently as both a sensor and an actuator, owing to the properties of the piezoelectric material phenomenon. Moreover, the EMI technique is distinguished by its extensive frequency spectrum, swift responsiveness, and, more significantly, costeffectiveness.

The EMI method leverages the intrinsic coupling characteristics of piezoelectric materials, such as lead zirconate titanate (PZT) transducers, to correlate the EMI response of an attached PZT transducer with the mechanical impedance structure. Specifically, the structural attributes of the monitoring structure, encompassing mass, stiffness, and damping, influence its mechanical impedance and are manifested in the EMI responses of the PZT patches [19]. Therefore, any variations in the structural integrity of the monitored structure are reflected in the EMI signature of the PZT [20]. Based on published literature, PZT transducers are typically integrated as smart aggregates within RC members [21] or affixed to their exterior surface using epoxy bonding [22]. However, according to Naoum et al., embedded PZT sensors, such as smart aggregates, exhibit heightened sensitivity to the accumulation of damage and the stress fields of the host structure when compared to externally bonded PZT patches [23]. Moreover, research has emphasized the influence of temperature fluctuations on the EMI response of PZT transducers; consequently, a compensation procedure is required to differentiate the impact of environmental factors such as temperature and humidity variations [24, 25].

Researchers have thoroughly investigated the efficacy of the EMI method for SHM of RC members over the last decade. The majority of studies focused on prompt load-

induced damage detection, yielding promising results [26, 27]. Furthermore, research initiatives have shown the applicability of the EMI method for SHM of full-scale subassemblies of RC structures, including RC beams [21, 28–30] and RC joints [31–33] under quasi-static loading. Recently, the SHM of retrofitted RC members using EMI-based methods has been carried out through the application of machine learning techniques [16, 17, 27]. However, previous research has primarily focused on damage detection using quasi-static loading conditions, and studies concerning the SHM of RC structures under dynamic loads remain notably limited.

Therefore, this study conducted an experimental investigation into the effectiveness of the EMI method for damage detection in a one-bay, one-story RC space frame structure subjected to seismic vibrations. Consequently, a 3d RC specimen has been fabricated with meticulously positioned PZT sensors. More specifically, the EMI responses of seven PZT sensors are illustrated, of which five have been mounted on a beam and two on a column. The RC specimen was subjected to incremental levels of Peak Ground Acceleration (PGA) on a shaking table. To accomplish this incremental loading, a spectrogram of the significant ground motion that notably affected Thessaloniki in 1978 was carefully modified, thereby subsequently determining the dynamic behavior of the shaking table. Between the seismic sequences, the EMI responses of the PZT transducers were recorded through a novel autonomous monitoring device. The EMI signatures obtained were employed to facilitate the prompt identification of damage within the RC columns during the shake table tests. The findings underscore the efficacy and sensitivity of the EMI-based methodology for the SHM of RC space frame structures subjected to seismic excitations.

# 2 Materials and Methods

## 2.1 Materials Properties

This study involved casting one 3d frame RC specimen at a scale of 3:1. The research employed a ready-mixed C20/25-grade concrete that complies with EN 206 standards. Furthermore, two types of steel reinforcement were employed. The slab, the foundation, and the longitudinal reinforcement of the columns utilized B500C, while the stirrups of the columns employed S220. Additionally, hollow clay bricks were employed for the construction of the masonry infills with dimensions 60/90/190 mm (width/height/length), a weight of about 1.2 kg per brick, and vertical holes covering 55% of the total brick volume. The nominal average axial compressive strength of bricks, as determined by the EN772-1 uniaxial compression test, with vertical holes, is approximately 9.8 MPa; when the percentage of holes is excluded, this value increases to 21.7 MPa.

Furthermore, PZT transducers were utilized in this investigation for EMI-based SHM. The PZT patches used in this publication are commercially supplied by Pi Ceramics and have dimensions of  $10 \text{ mm} \times 10 \text{ mm} \times 2 \text{ mm}$ , as depicted in Figure 2. According to the manufacturer's specifications, the density of the PZT was 7800 kg/m<sup>3</sup>. Furthermore, its Poisson's ratio is 0.34; the mechanical quality factor and the

dielectric loss factor are 100 and  $20 \times 10-3$ , respectively. Furthermore, the relative permittivity was measured to be 2400 and 1980 in the parallel and perpendicular orientations to the polarity, respectively.

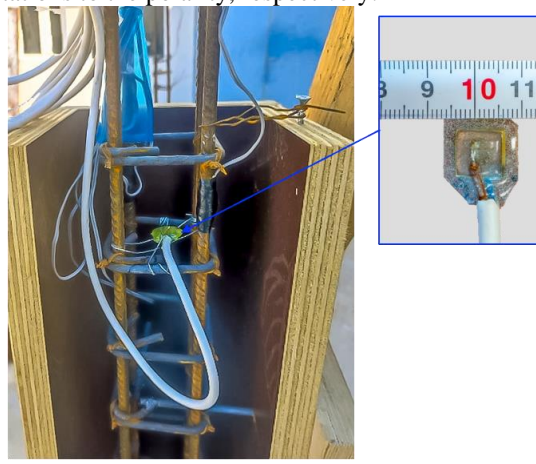


Fig. 2. Ready to install PZT Patch

#### 2.2 Specimens' details

As previously stated, the experimental investigation involves subjecting a one-bay, single-story RC frame structure to earthquake simulation through testing on a shaking table, with gradually increased Peak Ground Acceleration (PGA) level. The specimen was designed in accordance with older code provisions established in the 1970s, prior to the adoption of the current Eurocodes 2 and 8, as well as the New Greek Seismic Code for Concrete Structures. This choice is attributed to the fact that a significant portion of existing structures were designed and constructed prior to the establishment of modern codes. The structural components of the specimen consist of a slab with four cantilevers, four beams, four columns, and four infill masonry walls.

The clear span of the beams was 1.24 meters, while the clear height of the columns was 1.0 meters. The cross-section of the column measured 13 by 13 centimeters, with four longitudinal reinforcement bars, each with an 8-millimeter diameter, meticulously positioned at each corner. Additionally, a closed steel stirrup fabricated from a smooth S220 steel grade, with a diameter of 5.5 millimeters, was positioned every 6 centimeters to serve as a transverse component reinforcement. Furthermore, an RC slab featuring four balconies and four hidden beams was built atop the columns, with a thickness of 20 centimeters. This bulky RC slab was employed to concentrate the potential damage to the RC columns and the brick infill panels.

# 2.3 Testing procedure

As mentioned earlier, this study involves subjecting an RC frame structure to incremental levels of PGAs using a shaking table. The dynamic test was performed at the Laboratory of Reinforced Concrete and Seismic Design of Structures at Democri-

tus University of Thrace, situated in Xanthi, Greece. According to the manufacturer, the uniaxial acceleration capacity of the shake table was 1.6g for a payload mass of eight tons and 2.9g for a payload mass of four tons. Additionally, the maximum velocity and displacement of the shaking table were 1.2 m/sec and 23 centimeters, respectively. Furthermore, the range of response frequencies extended from 1.0 to 50.0 Hertz.

Additionally, 12 accelerometers, 8 string potentiometers, and 20 strain gauges were employed. To determine the story drift of the RC structure, 4 string potentiometers were employed. To evaluate the deformation associated with the in-plane response of the infills, 2 pairs of string potentiometers were utilized. The accelerometers were placed in triples to capture the three motion components. Furthermore, suitable markers for vision-based SHM were systematically positioned on the surfaces of the specimens. These markers were used to extract the displacement field from videos captured by two cameras arranged perpendicular to each other.

The dynamic loading testing encompassed a gradual increase of PGA levels until reaching a peak acceleration of 1.1g, utilizing the earthquake component from Thessaloniki in the north-south direction (peak acceleration of 0.14g). The earthquake transpired on 20 June 1978 at 20:03:21, at an epicenter located 30 kilometers east of Thessaloniki, thereby highlighting the vulnerability of urban centers to such natural disasters. According to the literature, 4000 buildings suffered severe damage, along with 13000 experiencing moderate damage and 49000 encountering minor damage [34]. More specifically, the excitation time history was generated based on the northsouth component of the seismic sequence, as recorded at the Thessaloniki-City Hotel station, located 29 kilometers from the epicenter, as depicted in Fig. 3. Subsequently, employing a dynamic pushover approach, this sequence has been carefully adjusted to induce the specimen with peak accelerations of up to 0.1 g, 0.2 g, 0.5 g, 0.8 g, and 1.1 g. The final stage of the initial testing phase of the as-built structure (as presented herein) was indicative of a structure equipped with RC members at Serviceability Limit States (SLS), where no yielding of steel rebars was observed, and brick infills exhibited damage initiation without collapse.

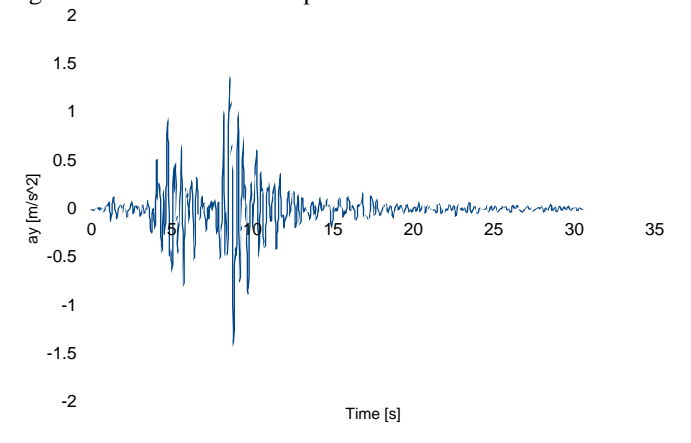


**Fig. 3.** The time history of ground acceleration during 1978 the Thessaloniki earthquake occurred on 20 June 1978.

#### 2.4 SHM procedure

This study experimentally investigates the efficacy of the EMI method for SHM of RC structures under dynamic loading. The EMI method leverages the piezoelectric phenomenon, which is the ability of piezoelectric materials to generate surface electric charges when subjected to mechanical stress and to undergo mechanical deformation when exposed to an electric field. Several scholars have examined the interaction between a mounted PZT transducer and the host structure, proposing analytical models to elucidate the EMI response of an attached PZT transducer subjected to harmonic excitation. According to Liang et al., the development of damage within an RC structure diminishes its mechanical impedance, which is subsequently reflected in the electrical impedance of an attached piezoelectric transducer [35]. Therefore, any variation in frequently captured EMI responses of a fixed PZT patch within a designated frequency band indicates the occurrence of structural damage in its vicinity.

Consequently, the mechanical properties, including mass, damping, and Young's modulus, are reflected in the EMI signature of PZT as a result of the interactions between the monitored structure and the PZT transducer. Therefore, any degradation in the mechanical properties of the host structures alters the electrical impedance of an attached PZT transducer. Therefore, substantial variations observed in the EMI response measurements indicate the potential occurrence of structural deterioration within the monitored infrastructure.

Scholars typically utilize statistical scalar indices, such as Correlation Coefficient Deviation (CCD) and Mean Absolute Percentage Deviation (MAPD), to assess damage derived from the EMI responses of smart aggregates. Nevertheless, this research utilized the Damage Index most frequently referenced in scholarly literature, the Root Mean Square Deviation (RMSD). The RMSD quantifies the variation between the EMI response in the pristine condition and after each loading sequence [36].

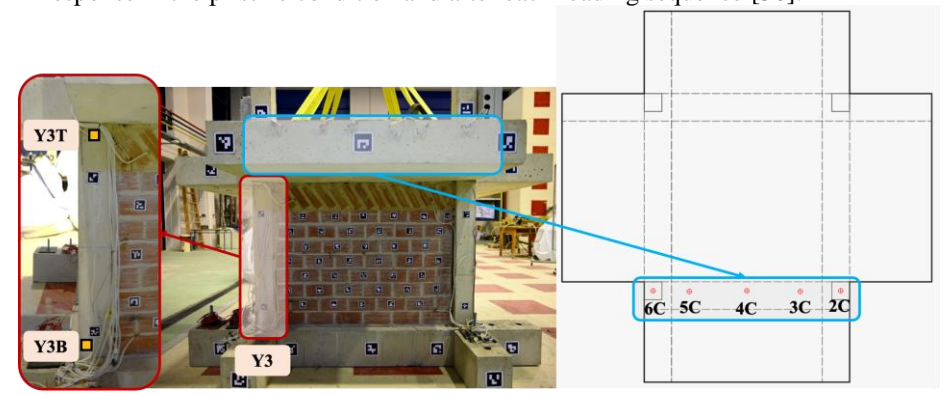


Fig. 4. Layout of PZT sensors in the 3d RC specimen.

For the SHM of the 3d RC frame structure, seven PZT transducers were placed as smart aggregates. As shown in Fig. 4two PZT sensors were placed in column Y3, one in each critical region of the column. Additionally, five PZT sensors were installed on beam C, beginning with PZT 2C at the joint of beams C and A, as well as column Y2. The PZT 3C was positioned approximately 30 centimeters from the joint of PZT 2C.

Then, the PZT 4C was placed in the midspan of beam C. Subsequently, PZT 6C and 5C were symmetrically positioned relative to PZT 2C and 3C at the intersection of beams C and B, as well as at column Y3. The EMI responses of all the PZTs were captured after each loading sequence.

# 3 Experimental Results

#### 3.1 The EMI response of PZT sensors

This sub-section delineates the EMI response of each PZT sensor in relation to Vp—excitation frequency, as recorded with the RC specimen at rest. The EMI responses were measured over a comprehensive frequency range from 10 to 250 kHz. The EMI response of the PZT sensors positioned in column Y3 is initially illustrated. Fig. 5 shows the EMI response of PZT Y3B, which was placed in the lower critical region of column Y3. Following the third test run, corresponding to a PGA of 0.5g, minor surface cracks were observed in the lower region of column Y3. These cracks propagated further during subsequent loading sequences. During the first two loading sequences, which correspond to 0.1 g and 0.2 g, the EMI response of the PZT Y3B remains unaltered. However, following the development of bending cracks near PZT Y3B, its EMI response demonstrates significant variability. Thus, the proposed SHM scheme promptly identifies the formation of a bending crack in the lower region of the column through alterations in the PZT Y3B EMI responses.

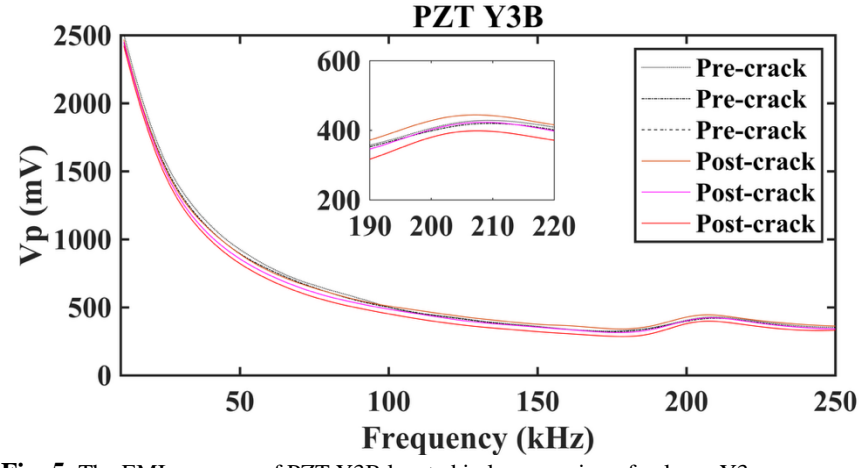


Fig. 5. The EMI response of PZT Y3B located in lower region of column Y3.

Following, the EMI responses of PZT Y3T are depicted in Fig. 6. PZT Y3T was positioned in the upper critical region of column Y3. However, no surface cracks have been observed in the upper region of the column throughout the testing procedure, in contrast with the lower area. The EMI response of PZT Y3T exhibits slight variations near its peak frequency. These findings imply the formation of small, scattered microcracks in the upper region of the Y3 column.

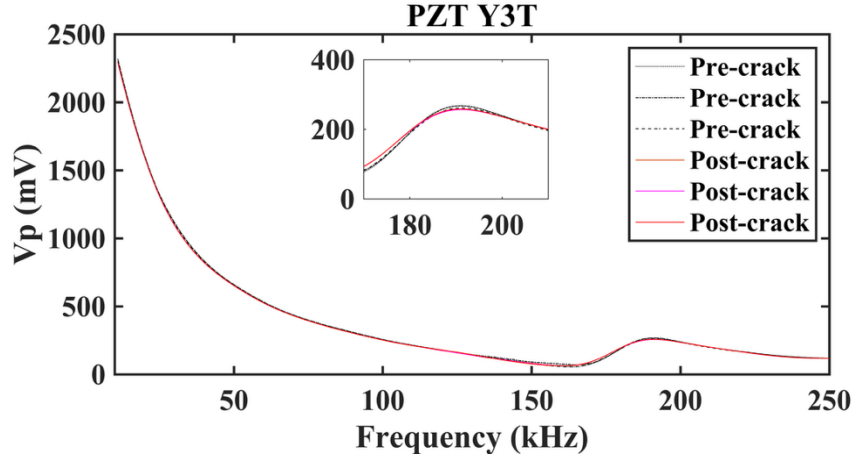
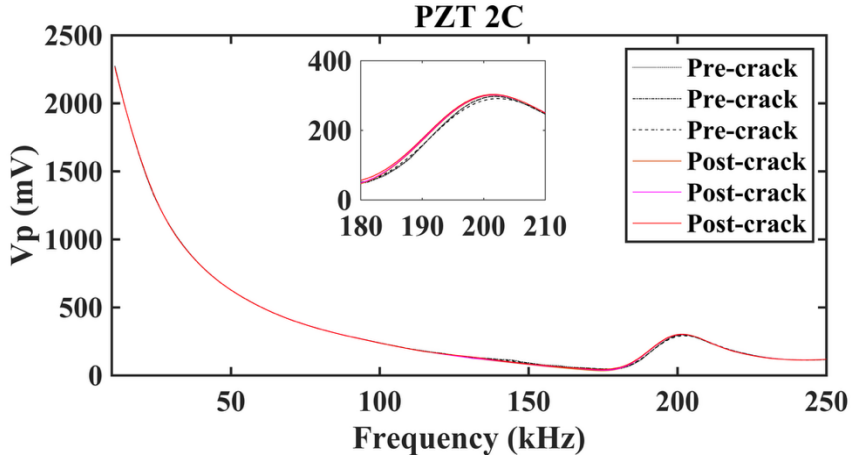


Fig. 6. The EMI response of PZT Y3T located in upper region of column Y3.

Subsequently, the EMI responses of the PZT sensors on beam B are illustrated. Fig. 7 illustrates the EMI response of PZT 2C, which was placed in the joint between column Y2 and beams C and A. The EMI response of PZT 2C exhibits a slight leftward shift, which, however, is not a significant variation. This signifies the commencement of microcrack formation within the joint region, although no surface cracks have been observed in the joint area. Thus, scattered internal microcracks may have been formed in its vicinity.



**Fig. 7.** The EMI response of PZT 2C located in RC Joint of the beam C and A. The EMI response of PZT sensor 3C is subsequently illustrated in Fig. 5. PZT 3C was positioned approximately 30 centimeters from the joint towards the midspan of the beam. The EMI response of PZT 3C does not show variation, implying that the area near the PZT transducer remained intact during the loading sequences.

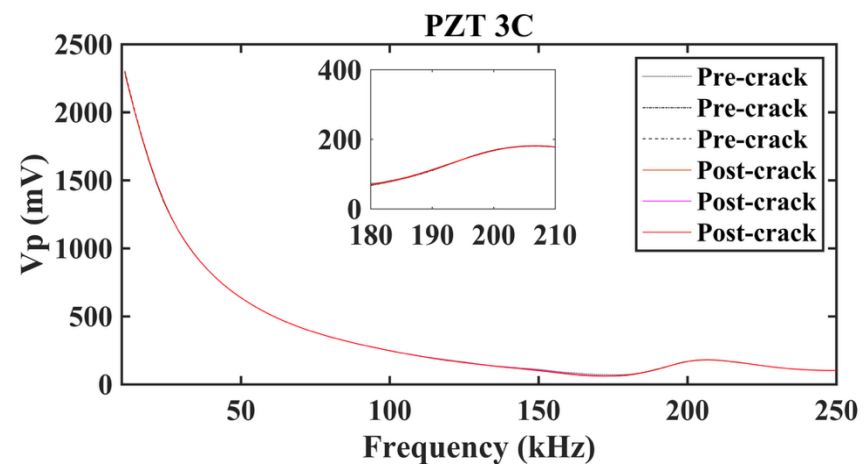


Fig. 8. The EMI response of PZT 3C.

Subsequently, Fig. 9 depicts the EMI response of PZT patch 4C. Although PZT 4C was situated at the midspan of beam C, no significant variations in the EMI responses were observed during the loading sequences. This implies that damage has not occurred in the midsection of beam C, according to the EMI method.

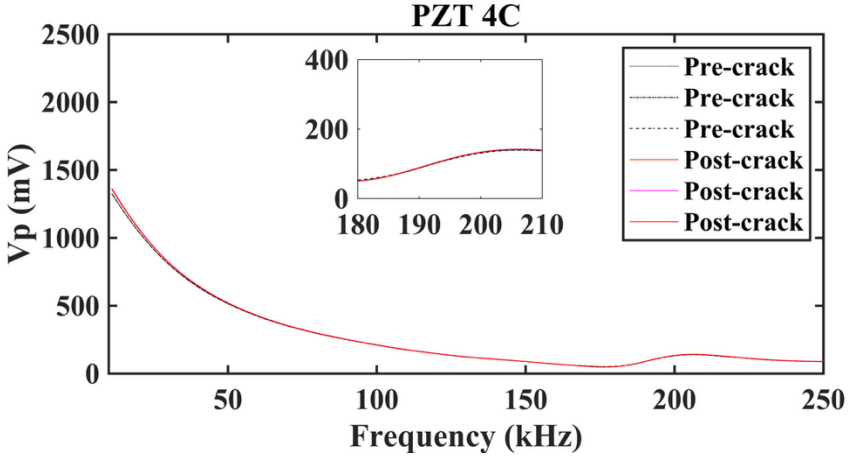


Fig. 9. The EMI response of PZT 4C.

Fig. 10 illustrates the EMI response of PZT 5C, which was placed symmetrically with respect to PZT 3C, 30 approximately 30 centimeters from the joint of beam C and B. Similarly, as with the preceding PZT sensors, the EMI response of PZT 5C does not exhibit significant variations, indicating that damage has not occurred in its vicinity.

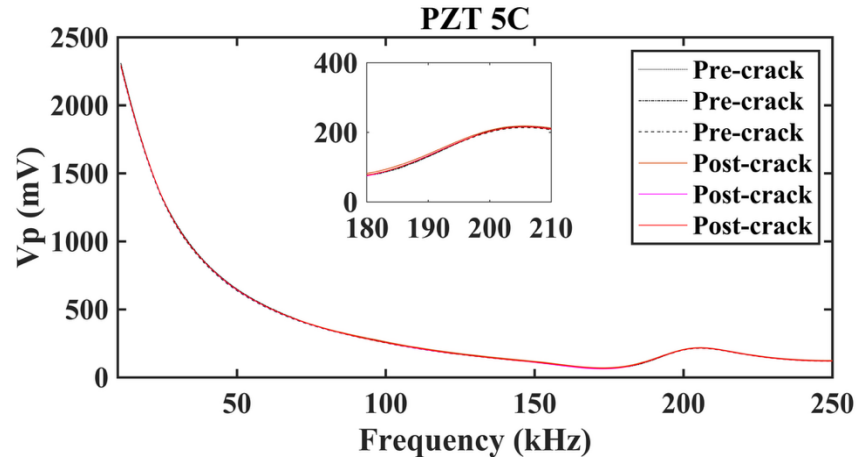
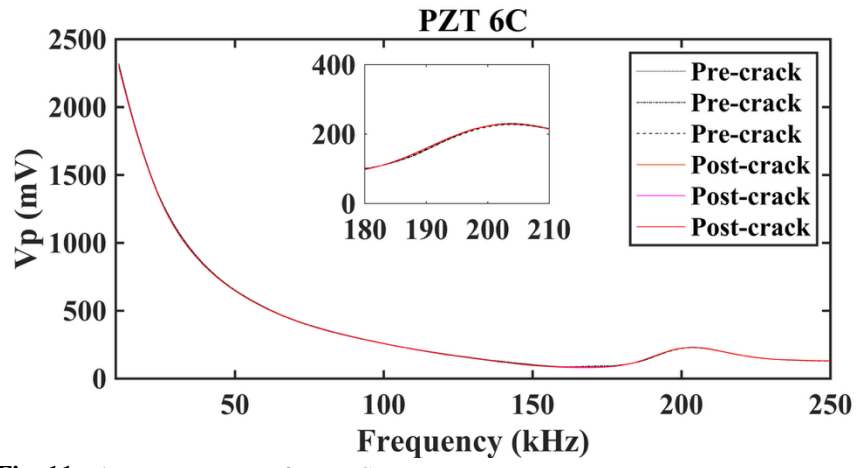


Fig. 10. The EMI response of PZT 5C.

Similarly, Fig. 11 illustrates the EMI response of PZT 6C, which was positioned at the joint between beam C and beam B, as well as the column Y3. In contrast to PZT 2C, the EMI response of PZT 6C remains unaltered throughout the loading process.



**Fig. 11.** The EMI response of PZT 6C.

#### 3.2 Quantification of EMI response variations

As previously mentioned, the RMSD damage index was employed to quantify the variations in the EMI responses of PZTs in this study. Fig. 12 depicts the RMSD values of the PZT sensors of column Y3. The RMSD values of PZT Y3B demonstrate a significant increase following the third loading sequence, rising from 2.5% to 3.6%, and then progressively advancing to 5.7% and 9.7% during the fourth and fifth loading sequences, respectively. The RMSD values of PZT Y1T also exhibit a slight in-

crease following the third loading test, rising from 0.9% to 1.6%, and persist throughout the loading process. These findings are consistent with the observed crack patterns in the column, whereby the fissure developed in its lower region. Thus, the proposed SHM scheme effectively detects the degradation of the structural integrity of the 3d frame structure.

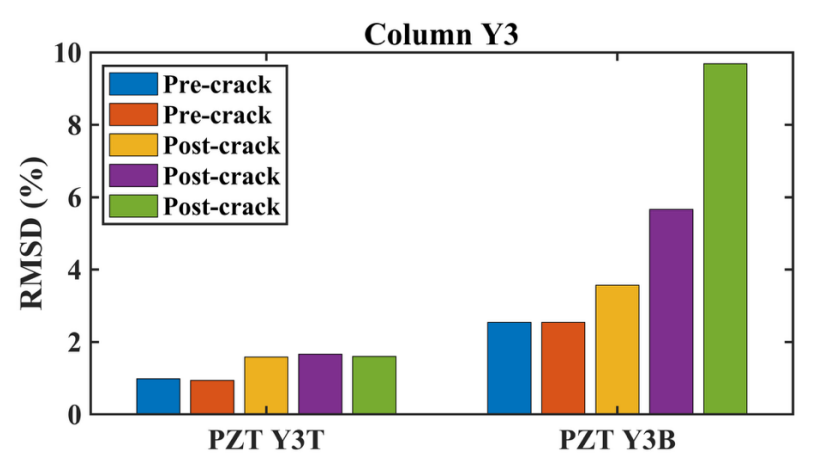


Fig. 12. The RMSD damage index values of PZT sensors of Column Y3.

Subsequently, the RMSD values of the PZT sensors of Beam C are depicted in Fig. 13. The RMSD values of all sensors on the beam vary between 0.3% and 2.1% during the loading tests. As anticipated, there was no significant damage to the beam due to the presence of the substantial reinforced concrete slab, which concentrated the damage within the vertical structural elements. This phenomenon is common in existing buildings constructed according to older standards, characterized by strong slabs or beams and relatively weaker columns.

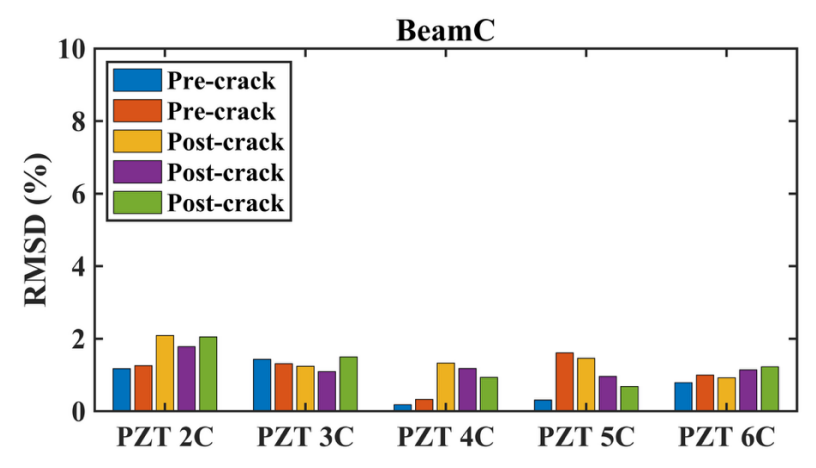


Fig. 13. The RMSD damage index values of PZT sensors of Beam C.

## 4 Conclusions

This study examines the feasibility of the EMI method for SHM of a single-bay, single-floor reinforced concrete frame structure subjected to seismic sequences. Therefore, PZT sensors were carefully positioned within an RC specimen, which was exposed to varying percentages of PGA from a significant seismic event. Thus, cracks were formed in the critical regions of the columns, and the masonry infills. This study classified the structural integrity of the RC specimen into two distinct categories: precrack and post-crack. The EMI method effectively identified crack formation by detecting variations in the EMI responses of the column PZT sensor, thereby demonstrating its feasibility for the SHM of RC structures. In contrast, the PZT sensors located in the beam, where cracks weren't formed, exhibit minor variations. Therefore, the proposed SHM scheme promptly identifies the initiation of damage formation, even though it was relatively close to the Serviceability Limit States (SLS) of RC structures. Such RC damages are difficult to detect, as the residual drift of the structure is negligible. Future research should further investigate the effectiveness of the EMI method under conditions approaching near-collapse damage in RC structures, as well as the effects resulting from additional mass following innovative renovations.

## Acknowledgment

The research project is implemented in the framework of H.F.R.I call "Basic research Financing (Horizontal support of all Sciences)" under the National Recovery and Resilience Plan "Greece 2.0" funded by the European Union—NextGenerationEU (H.F.R.I. Project Number: 015376). https://greenergy.civil.duth.gr/

## References

- Li Y, Wei M, Hu X (2023) Damage monitoring of the planting balcony in vertical greenery buildings using the EMI method. Smart Mater Struct 32:035038. https://doi.org/10.1088/1361-665X/acbcb2
- Kassem MM, Beddu S, Ooi JH, Tan CG, Mohamad El-Maissi A, Mohamed Nazri F (2021) Assessment of Seismic Building Vulnerability Using Rapid Visual Screening Method through Web-Based Application for Malaysia. Buildings 11:485. https://doi.org/10.3390/buildings11100485
- Mpalaskas AC, Matikas TE, Aggelis DG, Alver N (2021) Acoustic Emission for Evaluating the Reinforcement Effectiveness in Steel Fiber Reinforced Concrete. Applied Sciences 11:3850. https://doi.org/10.3390/app11093850

- Li P, Zhang W, Ye Z, Wang Y, Yang S, Wang L (2022) Analysis of Acoustic Emission Energy from Reinforced Concrete Sewage Pipeline under Full-Scale Loading Test. Applied Sciences 12:8624. https://doi.org/10.3390/app12178624
- Erdogmus E, Garcia E, Amiri AS, Schuller M (2020) A Novel Structural Health Monitoring Method for Reinforced Concrete Bridge Decks Using Ultrasonic Guided Waves. Infrastructures 5:49. https://doi.org/10.3390/infrastructures5060049
- Olisa SC, Khan MA, Starr A (2021) Review of Current Guided Wave Ultrasonic Testing (GWUT) Limitations and Future Directions. Sensors 21:811. https://doi.org/10.3390/s21030811
- Sony S, Laventure S, Sadhu A (2019) A literature review of next-generation smart sensing technology in structural health monitoring. Struct Control Health Monit 26:e2321. https://doi.org/10.1002/stc.2321
- 8. Maru MB, Lee D, Tola KD, Park S (2020) Comparison of Depth Camera and Terrestrial Laser Scanner in Monitoring Structural Deflections. Sensors 21:201. https://doi.org/10.3390/s21010201
- Halabe UB, Vasudevan A, Klinkhachorn P, GangaRao HVS (2007) Detection of subsurface defects in fiber reinforced polymer composite bridge decks using digital infrared thermography. Nondestructive Testing and Evaluation 22:155–175. https://doi.org/10.1080/10589750701448381
- Wei Z, Fernandes H, Herrmann H-G, Tarpani JR, Osman A (2021) A Deep Learning Method for the Impact Damage Segmentation of Curve-Shaped CFRP Specimens Inspected by Infrared Thermography. Sensors 21:395. https://doi.org/10.3390/s21020395
- 11. Lee JY, Sim C, Detweiler C, Barnes B (2019) Computer-Vision Based UAV Inspection for Steel Bridge Connections. In: Structural Health Monitoring 2019. DEStech Publications, Inc.
- Won K, Sim C (2020) Automated Transverse Crack Mapping System with Optical Sensors and Big Data Analytics. Sensors 20:1838. https://doi.org/10.3390/s20071838
- Kumarapu K, Mesapam S, Keesara VR, Shukla AK, Manapragada NVSK, Javed B (2022) RCC Structural Deformation and Damage Quantification Using Unmanned Aerial Vehicle Image Correlation Technique. Applied Sciences 12:6574. https://doi.org/10.3390/app12136574
- Perera R, Huerta MC, Baena M, Barris C (2023) Analysis of FRP-Strengthened Reinforced Concrete Beams Using Electromechanical Impedance Technique and Digital Image Correlation System. Sensors 23:8933. https://doi.org/10.3390/s23218933

- Papadopoulos NA, Naoum MC, Sapidis GM, Chalioris CE (2024) Resilient and Sustainable Structures through EMI-Based SHM Evaluation of an Innovative C-FRP Rope Strengthening Technique. Applied Mechanics 5:405–419. https://doi.org/10.3390/applmech5030024
- Sapidis GM, Kansizoglou I, Naoum MC, Papadopoulos NA, Chalioris CE (2024) A Deep Learning Approach for Autonomous Compression Damage Identification in Fiber-Reinforced Concrete Using Piezoelectric Lead Zirconate Titanate Transducers. Sensors 24:386. https://doi.org/10.3390/s24020386
- 17. Perera R, Torres L, Ruiz A, Barris C, Baena M (2019) An EMI-Based Clustering for Structural Health Monitoring of NSM FRP Strengthening Systems. Sensors 19:3775. https://doi.org/10.3390/s19173775
- Ai D, Zhang D, Zhu H (2024) Damage localization on reinforced concrete slab structure using electromechanical impedance technique and probability-weighted imaging algorithm. Construction and Building Materials 424:135824. https://doi.org/10.1016/j.conbuildmat.2024.135824
- Kocherla A, Duddi M, Subramaniam KVL (2021) Embedded PZT sensors for monitoring formation and crack opening in concrete structures. Measurement 182:109698. https://doi.org/10.1016/j.measurement.2021.109698
- Bhalla S, Soh CK (2004) Electromechanical Impedance Modeling for Adhesively Bonded Piezo-Transducers. Journal of Intelligent Material Systems and Structures 15:955–972. https://doi.org/10.1177/1045389X04046309
- Papadopoulos NA, Naoum MC, Sapidis GM, Chalioris CE (2023) Cracking and Fiber Debonding Identification of Concrete Deep Beams Reinforced with C-FRP Ropes against Shear Using a Real-Time Monitoring System. Polymers 15:473. https://doi.org/10.3390/polym15030473
- Liang C, Sun F, Rogers CA (1996) Electro-mechanical impedance modeling of active material systems. Smart Mater Struct 5:171–186. https://doi.org/10.1088/0964-1726/5/2/006
- Naoum MC, Sapidis GM, Papadopoulos NA, Voutetaki ME (2023) An Electromechanical Impedance-Based Application of Realtime Monitoring for the Load-Induced Flexural Stress and Damage in Fiber-Reinforced Concrete. Fibers 11:34. https://doi.org/10.3390/fib11040034
- 24. Parpe A, Saravanan TJ (2021) New refined analytical models for various bonding conditions of an adhesively bonded smart PZT transducer using the EMI technique. Smart Mater Struct 30:125015. https://doi.org/10.1088/1361-665X/ac32e9

- Haider MF, Giurgiutiu V, Lin B, Yu L (2017) Irreversibility effects in piezoelectric wafer active sensors after exposure to high temperature. Smart Mater Struct 26:095019. https://doi.org/10.1088/1361-665X/aa785f
- Sapidis GM, Naoum MC, Papadopoulos NA (2025) Electromechanical Impedance-Based Compressive Load-Induced Damage Identification of Fiber-Reinforced Concrete. Infrastructures 10:60. https://doi.org/10.3390/infrastructures10030060
- Ai D, Mo F, Han Y, Wen J (2022) Automated identification of compressive stress and damage in concrete specimen using convolutional neural network learned electromechanical admittance. Engineering Structures 259:114176. https://doi.org/10.1016/j.engstruct.2022.114176
- 28. Ai D, Luo H, Wang C, Zhu H (2018) Monitoring of the load-induced RC beam structural tension/compression stress and damage using piezoelectric transducers. Engineering Structures 154:38–51. https://doi.org/10.1016/j.engstruct.2017.10.046
- Naoum MC, Papadopoulos NA, Sapidis GM, Chalioris CE (2024) Advanced Structural Monitoring Technologies in Assessing the Performance of Retrofitted Reinforced Concrete Elements. Applied Sciences 14:9282. https://doi.org/10.3390/app14209282
- Angeli GM, Naoum MC, Papadopoulos NA, Kosmidou P-MK, Sapidis GM, Karayannis CG, Chalioris CE (2024) Advanced Structural Technologies Implementation in Designing and Constructing RC Elements with C-FRP Bars, Protected Through SHM Assessment. Fibers 12:108. https://doi.org/10.3390/fib12120108
- 31. Sapidis GM, Naoum MC, Papadopoulos NA, Golias E, Karayannis CG, Chalioris CE (2024) A Novel Approach to Monitoring the Performance of Carbon-Fiber-Reinforced Polymer Retrofitting in Reinforced Concrete Beam–Column Joints. Applied Sciences 14:9173. https://doi.org/10.3390/app14209173
- Divsholi BS, Yang YW, Bing L (2009) Monitoring Beam-Column Joint in Concrete Structures Using Piezo-Impedance Sensors. AMR 79–82:59–62. https://doi.org/10.4028/www.scientific.net/AMR.79-82.59
- 33. Naoum M, Sapidis G, Papadopoulos N, Golias E, Chalioris C (2023) Structural Health Monitoring of Reinforced Concrete Beam-Column Joints Using Piezoelectric Transducers. In: Jędrzejewska A, Kanavaris F, Azenha M, Benboudjema F, Schlicke D (eds) International RILEM Conference on Synergising Expertise towards Sustainability and Robustness of Cement-based Materials and Concrete Structures. Springer Nature Switzerland, Cham, pp 945–956
- 34. Theodulidis N, Roumelioti Z, Panou A, Savvaidis A, Kiratzi A, Grigoriadis V, Dimitriu P, Chatzigogos T (2006) Retrospective Prediction of Macroseismic Intensities Using Strong

- Ground Motion Simulation: The Case of the 1978 Thessaloniki (Greece) Earthquake (M6.5). Bull Earthquake Eng 4:101-130. https://doi.org/10.1007/s10518-006-9001-6
- 35. Liang C, Sun FP, Rogers CA (1997) An Impedance Method for Dynamic Analysis of Active Material Systems. Journal of Intelligent Material Systems and Structures 8:323–334. https://doi.org/10.1177/1045389X9700800405
- Naoum MC, Papadopoulos NA, Sapidis GM, Voutetaki ME (2024) Efficacy of PZT Sensors Network Different Configurations in Damage Detection of Fiber-Reinforced Concrete Prisms under Repeated Loading. Sensors 24:5660. https://doi.org/10.3390/s24175660